Adsorption, Vibration, and Diffusion of O Atoms on Rh Low-Index and (711) Stepped Defective Surfaces

Zhao Yu Diao,[†] Ce Hao,[‡] Ze Xin Wang,*[,†] Chen Chu Dong,[†] and Xue Hui Pang[†,§]

Department of Chemistry, Shandong Normal University, Jinan 250014, China, Department of Chemistry, Dalian University of Technology, Dalian 116024, China, and Ocean University of China, Qingdao, China

Received: January 19, 2005; In Final Form: May 9, 2005

The adsorption, vibration, and diffusion of O atoms on Rh(100), Rh(111), Rh(110), and Rh(711) surfaces were studied using the 5-parameter Morse potential (5-MP) of interaction between an adatom and a metal surface cluster. Our theoretical calculations provide information about adsorption sites, adsorption geometry, binding energy, and eigenvibration. Our results agreed very well with experimental results. Four major results follow. First, the theoretical calculation showed that on the Rh(100) surface the 4-fold hollow site is the only adsorption site. Second, on the O−Rh(111) system, the 3-fold hollow site is the stable adsorption site. Third, on the Rh(110) surface at low coverage, the O atom is adsorbed preferably on the pseudo-3-fold site, while with increasing coverage, the O atom is adsorbed not only on the pseudo-3-fold site but also on the long bridge site. Last, as for the Rh(711) stepped surface, the 3-fold site on the (111) step is metastable, whereas the 4-fold sites on the (100) terrace are stable, which enables the O atoms to diffuse easily from the 3-fold to the 4-fold site at low coverage. Therefore, the O atoms are adsorbed preferrably on the stable 4-fold sites of the (100) terrace and then later as coverage increases on the metastable 3-fold site of the (110) step.

Introduction

The interaction between the O atom and the metal is the essential influencing factor in the processes of growth, oxidation, and corrosion of surfaces and the heterogeneous catalysis of the metal surface cluster. The adatom O affects the activity and selectivity of catalytic transition-metal crystal surfaces,[1] so the precise determination of the adsorption geometry of the atoms, the molecules, and the molecule fragments is one of the key processes in explaining catalytic activity and selectivity.[2] Rh is one of the widely used noble metal catalysts and is applied especially to automotive catalytic converters.[3] Therefore, great interest in the study of the O−Rh system is arising. Many investigations have been performed on the O−Rh system by experimental techniques, such as electron energy loss spectroscopy (EELS),[3,6,15−18] low energy electron diffraction (LEED),[3−14,17,28] and Auger electron spectroscopy (AES).[3,6,17] Theoretical computations, such as the density functional theory (DFT),[1,21−26] have been used as well.

Hansen[1] et al. studied the adsorption of O atoms on Rh(100) with DFT. They pointed out that serious reconstruction existed on the Rh(100) surface and that there was a strong tendency for oxygen to be adsorbed in the 3-fold site on all of the Rh surfaces. They carried out theoretical calculations and predicted that the O atom is adsorbed in the 4-fold hollow site. The calculations showed that the bond length of the 4-fold state is 2.17 Å, and the binding energy for the O atom is 5.2 eV.

A LEEDI-V experiment was also carried out by Baraldi et al.[4] to investigate the adsorption of the O atom on Rh(100). The results indicate that the O atom is adsorbed in the 3-fold of rhombi shapes created by the reconstruction of the first layer of rhodium, with minimum bond lengths of 2.02 and 2.09 Å and an adsorption height of 1.05 Å.

However, by using surface X-ray diffraction (SXRD), the experimental results of Norris et al.[19] on the O atom inducing reconstruction on Rh showed that the Rh atoms in the exterior layer adopt a "clock" reconstruction, and that the O atom is situated in the "diamond" site rather than in the rotated 4-fold hollow site, with an adsorption height of 0.64 Å.

Dubois et al.[6] studied the ordered adsorption of the O atom on Rh(100) at 300 K combining the HREELS, LEED, and AES techniques. They conceived that the O atom occupies the highest coordination site (namely, the 4-fold hollow site) when both the disordered and ordered p(2 × 2) surface phases are formed. There was only a sort of 50−51 meV vibration frequency on the HREELS, which was assigned to the perpendicular vibration frequency of the 4-fold site by analogy.[7,27]

Root[15,16] et al. obtained 65.7[15] meV vibration frequency of the O atom on Rh(111) at 485 K with high coverage via EELS. At 470 K, they only got a 66.9 mV on the EELS and identified it as a vibration of O−Rh, without pointing out the exact adsorption site and vibration mode.

Alfe[17] et al. studied the order and disorder adsorption of the O atom on Rh(110) by HREELS, LEED, and AES. The experimental results showed that the single 72 meV was observed when the adatoms were in disorder at 90−120 K and at low coverage. With increasing coverage, the (2 × 1) p2mg surface formed, and two vibration frequencies, 45 and 63 meV, were observed. As the temperature was rising, the (2 × 3) p2mg, c (2 × 2*n*) phase formed, and the observed frequencies were 47 and 65 meV, respectively. Meanwhile, no vibration frequencies except for 65 meV appeared as the adatoms formed the (2 × 2) p2mg phase. They assigned the 72-meV vibration frequency to the long-bridge site, and the 63- and 45-meV frequency to the perpendicular and parallel vibration frequencies of the psuedo-3-fold site, respectively.

* Corresponding author. E-mail address: wangzexin@sdnu.edu.cn.
[†] Shandong Normal University.
[‡] Dalian University of Technology.
[§] Ocean University of China.

10.1021/jp0503258 CCC: $30.25
Published on Web 06/08/2005

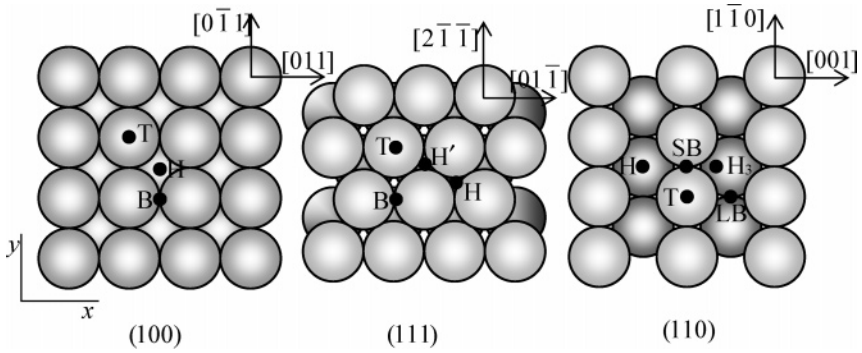

Figure 1. Surface sites are illustrated on Rh(100), (111), and (110). Shaded circle, Rh atom; Black dot, adsorption site; T, top site; B, bridge site; H, hollow site (fcc hollow site for Rh (111)); H′, hcp hollow site; H_3, pseudo-3-fold hollow site; LB, long-bridge site; SB, short-bridge.

Chang Q. Sun[28] et al. performed an investigation of the O atom on Rh(110) by the model of bond-to-bond and the potential-barrier. Their research indicated that the O atom occupied the 4-fold hollow site randomly. The monolayer adsorption of O atoms resulted in the missing-row reconstruction at the proper coverage ($\theta \leq 0.5$), whereas the O atom was adsorbed on the psuedo-3-fold site when the adsorption height was 0.5−0.6 Å and the bond-length of the O atom and the first layer of Rh was 2.04−2.07 Å.

Cautero[18] et al. analyzed the adsorption and dissociation of O_2 on Rh(110) with HREELS. The experiment revealed only 68.2−70.7 meV on the loss spectroscopy at low coverage, and this decreased to 62.0 meV as the coverage increased. However, they did not designate a reasonable adsorption site.

The open stepped defective surface has attracted many scientists. Belton[3] et al. put forward a comprehensive and systematic investigation in the practice of the O atom on Rh-(711) with a broad range of coverage by means of LEED, HREELS, TPD, and AES. The results showed that three kinds of loss spectra of 410−435 cm^{-1} (∼50.8−53.9 meV), 500−550 cm^{-1} (∼61.2−68.2 meV), and 975−1079 cm^{-1} (120.9−133.8 meV) were observed on the HREELS and four varieties of desorption states (α_1, α_2, β_1, and β_2) appeared on the TPD diagram. They pointed out that 410−435 cm^{-1} (∼50.8−53.9 meV) was the stretch vibration frequency of the 4-fold site from the dissociated O atom on the (100) terrace and corresponded to the β_2 state on the TPD; however, 500−550 cm^{-1} (∼61.2−68.2 meV) was assigned to the 3-fold site on the (111) step surface that corresponded to the β_1 state. The adsorption of O_2 on the (111) step surface produced the 975−1079 cm^{-1} (120.9−133.8 meV) vibration frequency that corresponded to the α_2 state. The vibration frequency arising from the adsorption of O_2 on the (100) terrace was not measured.[3] They also pointed out that the dissociation of O_2 on the surface was very effortless at low temperatures with low coverage. Contrary to the former research outcome, the adsorption sequence was reversed; the dissociated O atom was first adsorbed on the 4-fold site on the (100) terrace and then on the 3-fold (111) step site.

All of these experimental and theoretical results lead us to an unanswered question: Why are the oxygen atoms first adsorbed on the 4-fold sites on the (100) terrace at low coverage but not on the active 3-fold sites on the (111) step? The resolution of this problem still needs considerable understanding of low index surfaces. So far, there has been no experimental or theoretical result for this aspect. Therefore, one purpose of this work is to figure out how to obtain all of the critical characteristic data of low index surfaces and sequentially obtain the necessary information in order to solve the above-mentioned problem. This work puts forward a theoretical method that utilizes the 5-parameter Morse potential of interaction between adsorbed O atoms and Rh surfaces. The method optimizes five parameters based on the aforementioned experimental data, obtains the total critical characteristics of the adatoms, and studies the microscopic dynamic properties of the O−Rh system. The method has already been used successfully to deal with O−Cu,[31] O−Pd,[32] and O−Ni[33] low index surfaces and O−Cu (211), (410),[31] O−Pd(311),[32] O−Ni(510), and (115)[33] stepped surface systems and has presented satisfactory experimental and theoretical results.

1. Theoretical Calculation Methods and Surface Cluster Models. 1.1 Theoretical Calculation Method, 5-MP. In our previous works,[31−33] the 5-MP method has been used successfully to deal with the interaction between adatoms and surfaces. An assumption called the "frozen surface approximation" was adopted; in other words, the positions of the atoms of the metal surface were fixed. The total potential energy $V(\vec{R})$ for the adatom and the whole surface cluster can be expressed as follows

$$V(\vec{R}) = \sum_{i=1}^{\text{cluster}} D\left(\frac{h_i + Q_1}{R_i + Q_2}\right)\{\exp[-2\beta(R_i - R_0)] - 2\exp[-\beta(R_i - R_0)]\}$$

in which R_i is the distance between the adsorbed atom and the *i*-th surface atom; h_i is the vertical distance between the adsorbed atom and the surface where the *i*-th metal atom lies; β and R_0 are the parameters for vibration and equilibrium distance, respectively; D is a simulating energy parameter; and Q_1 and Q_2 are two simulation parameters. This work employs such a method to deal with the binding energy in order to take into account the orientation affect of d electrons of transition metals. The potential function $V(\vec{R})$ consists of only 5 parameters: D, β, R_0, Q_1, and Q_2; therefore, the potential function $V(\vec{R})$ constructed in this way is called the 5-parameter Morse potential of the interaction between an adatom and a metal surface (5-MP).

1.2. Cluster Models for Rh Surfaces. Rhodium in its crystalline state belongs to the fcc lattice category with a lattice constant of $a_0 = 0.3796$ nm. Figure 1 shows cluster models and adsorption sites for Rh(100), (111), and (110). Having considered the local geometrical symmetry in a point group, the displacement symmetry for a surface crystal cell, and the boundary effect of adatoms, this work chose to simulate the Rh surfaces by using an Rh cluster of at least 5 layers of cell atoms. Each layer is at least 6 (length) × 6 (width) atoms and contains about 300 Rh atoms. Using this many atoms prevented the boundary inaccuracies that smaller clusters could have caused.

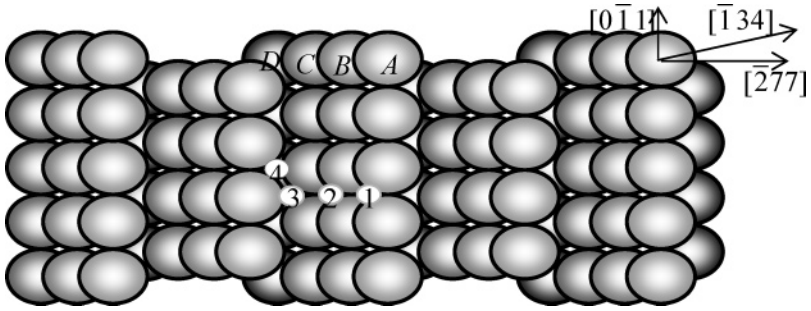

Figure 2. Structure and adsorption sites of Rh(711) stepped defective surface.

TABLE 1: Five Parameters for O−Rh Systems

system	D (eV)	β (Å^{-1})	R_0 (Å)	Q_1 (Å)	Q_2 (Å)
O−Rh	1.17	2.35	2.12	1.36	0.455

Figure 2 shows the cluster model and adsorption sites for the Rh(711) stepped surface. In Figure 2, the layer labeled A is the first Rh layer, and the layers labeled B, C, and D are the second, third, and fourth layers, respectively. Four kinds of nonequivalent sites denoted by 1, 2, 3, and 4, respectively, are contained in the cluster model. Therefore, the adsorption sites of 1, 2, and 3 are 4-fold sites and 4 is a 3-fold site. Because of the poor local geometrical symmetry of the crystal cell, this work simulated an Rh(711) surface by using an Rh cluster with 8 layers of cell atoms with every layer containing at least 10 (length) × 10 (width) atoms generally. This work took the [$\bar{2}$77] direction for x, the [0$\bar{1}$1] direction for the y axis, and the center of the T site for the coordinate zero.

We employed the experimental data of the three low-index Rh surfaces, (100), (110), and (111), to adjust the five parameters for the O−Rh interaction system as listed in Table 1. The kinetic characteristics of adsorption, such as the adsorption sites, adsorption geometry, binding energy, eigenvibration, and so forth, for an O atom on the three Rh low-index surfaces, (100), (110), and (111), obtained with our theoretical method were in good agreement with the experimental data. The investigation of the stepped defective surface systems O−Rh-(711) also provided credible results.

2. Results. Using the 5-MP method, we performed a systematic investigation of low-index Rh surfaces and obtained the complete critical characteristics of the O−Rh system. The calculation results are listed in Table 2. We applied the number of negative eigenvalues, which is denoted as λ, from the Hessian matrix to characterize the nature of the critical points. The Hessian matrix is obtained from the second derivative of $V(\vec{R})$. The critical point of $\lambda = 0$ is the minimum point for the surface adsorption state. The critical point of $\lambda = 1$ is the saddle point of the potential energy surface diffusion transitional state. The critical point of $\lambda = 2$ is the maximum point of surface diffusion ($\lambda = 2$ appears to be a second-order saddle point and not a true potential surface maximum). The case of $\lambda = 3$ does not exist on the cluster surface. N denotes the number of Rh atoms close to an O atom. E_b, f, R_{O-Rh}, and Z denote the binding energies, eigenvibration frequencies ($f_{||}$ and $f_{\perp}$ denote parallel and perpendicular vibration frequencies, respectively), bond length, and the vertical distance between O atoms and the cluster surface, respectively. A comparison between our results and the values from previous references is shown in Table 3.

2.1. O-Rh(100) System. On the Rh(100) surface, our results show that the crystal cell has three kinds of nonequivalent critical points corresponding to three kinds of nonequivalent adsorption sites, respectively. From the calculation results in Table 2, the top site, T, of $\lambda = 2$ is the surface diffusion maximum point, the bridge site, B, of $\lambda = 1$ is the surface diffusion transitional state, and the 4-fold hollow site, H, of $\lambda = 0$ is the surface adsorption state. Apparently, the surface adsorption state is the 4-fold hollow site, which also supports the prediction of Dubois[6] and Norris[19] et al. The binding energy of the adsorption state in our work is 4.69 meV, which is also in agreement with other experimental[21,34−37] and theoretical[1,22] results. In addition, the adsorption geometry with the optimal height of 1.06 Å and the bond length of 2.174 Å in our work has also been demonstrated by further experiments[4,5] and theoretical works.[1,5,22,26]

The 4-fold hollow site of the Rh(100) system has a C_{4v} local geometrical symmetry. The 46 meV eigenvibration is perpendicular to the surface and corresponds to the full-symmetrical A_1 irreducible representation. The 52 meV eigenvibration is parallel to the surface and corresponds to the 2D E degenerate irreducible representation. The perpendicular vibration frequency is generally lower than the parallel vibration frequency when oxygen resides in the 4-fold hollow site on Rh(100).[31−33] Dubois[6] et al. gained only one kind of loss spectra of 50−51.44 meV with HREELS and assigned it to the perpendicular vibration mode by analogy.[7,27] The perpendicular vibration frequency (44.51 meV) of the 4-fold state in our work agrees with their experimental results.[6]

2.2. O-Rh(111) System. Compared with other low-index surfaces, Rh(111) has the most compact surface and its crystal cell has a C_{3v} local geometrical symmetry. From the results shown in Table 2, there are four kinds of nonequivalent critical points on the surface (as shown in Figure 1): both 3-fold hollow sites fcc (H) and hcp (H′) are surface adsorption states with $\lambda = 0$; B is the surface diffusion transitional state between H and H′, and T is the surface diffusion maximum point. According to the Rh(111) surface structure, H′ and H are nonequivalent; however, the difference between their critical characteristics is very little in our calculations, as indicated by the nearly similar f, R_{O-Rh}, and Z_{O-Rh} values. The small discrepancy in the binding energies (0.01 eV) is difficult to identify by experiment so the values may be considered to be approximately equivalent.

From Table 3, all of the critical characteristics, such as binding energy and adsorption geometry, are consistent with many previous experimental and theoretical results.[7,9,12,13,15,16,22−25,36,38−40] The 3-fold hollow site has a C_{3v} local geometrical symmetry. The results in this work show that the eigenvibration of 72 meV is perpendicular to the surface and corresponds to the full-symmetrical A_1 irreducible representation. The vibration mode of 50 meV is parallel to the surface and corresponds to the degenerate E irreducible representation. Because the experimental results of 66−67 meV[15,16] agree with the calculations in this work, we have determined the 3-fold hollow site to have a perpendicular vibration frequency.

2.3. O-Rh(110) System. The Rh(110) surface is a zigzag surface made up of two (111) facets colliding with each other

TABLE 2: Critical Characteristics of O−Rh Surface Systems

					f (meV)			
O−Rh	system site	N	λ	E_b (eV)	∥	⊥	R_{O-Rh} (Å)	*Z* (Å)
(100)	H	4	0	4.90	73.55 × 2	44.51	2.10 × 4	0.92
	B	2	1	3.22	60.44	72.28	2.09 × 2	1.61
	T	1	2	2.07		76.75	2.08	2.08
(111)	H	3	0	4.23	53.96 × 2	72.44	2.12 × 3	1.44
	H′	3	0	4.24	54.15 × 2	72.51	2.12 × 3	1.44
	B	2	1	3.65	65.06	75.66	2.08 × 2	1.59
	T	1	2	2.23		78.85	2.07	2.07
(110)	H	1	2	4.36		82.48	2.08	0.73
	H_3	3	0	4.41	32.57, 28.63	77.44	2.19 × 2, 2.09	0.72
	LB	4	0	4.40	125.8, 16.47	45.12	1.95 × 2, 2.22 × 2	0.43
	S	2	1	4.38	28.26	80.32	2.21, 2.08	0.72
	SB	2	1	3.01	59.72	71.05	2.10 × 2	1.62
	T	1	2	1.90		74.51	2.09	2.09
(711)	H_1	4	0	4.85	73.87, 73.60	43.98	2.09 × 2, 2.11 × 2	0.63(0.75)[a]
	H_2	4	0	4.85	73.75, 73.54	44.00	2.09 × 2, 2.11 × 2	0.09(0.75)[a]
	H_3	4	0	5.08	71.05, 72.43	43.68	2.12 × 2, 2.10 × 2	−0.43(0.77)[a]
	H_4	3	0	3.80	50.32, 46.12	70.11	2.10 × 2, 2.12	0.53(1.38)[b]
	B_{12}	2	1	3.19	60.14	71.91	2.10 × 2	1.03
	B_{23}	2	1	3.20	60.07	71.85	2.10 × 2	0.51
	B_{34}	2	1	3.49	47.05	76.09	2.10, 2.09	0.41
	B_{41}	2	1	3.18	60.12	72.06	2.09, 2.10	1.32

[a] The value in parentheses is the adsorption height of O atoms above the (100) terrace. [b] The value in parentheses is the adsorption height of O atoms above the (111) step.

TABLE 3: Comparison between Our Results and References

	systems	experimental data	theoretical calculation	this work
R_{O-Rh} (Å)	(100) H	2.13[5]	2.17[1,22] 2.12[5]	2.10 × 4
	(110) H_3	1.97 × 2, 2.04[11]	2.00 × 3, 1.99 × 2, 2.06[20]	2.19 × 2
		1.86 × 2, 2.07[12]	(1.86−1.97) × 2, 2.04−2.07[28]	2.09
		1.90 × 2, 2.06 [13]		
		2.0 ± 0 × 10[14]		
	(110) SB	2.0[12]		2.10
	(111) H	2.00[8], 1.98[9,12]	2.00, 1.95, 1.98[24]	2.12 × 3
		2.01 × 2, 1.92 [13]	2.00[2] 2.02[23]	
			2.11 × 2, 1.55, 2.20 × 2, 1.67[34]	
			1.94−1.97[25]	
Z_{O-Rh} (Å)	(100) H	0.95[20], 1.05[13]	1.00[38] 0.98−1.06[40]	0.92
	(110) H_3	0.5−0.6[28]	0.60, 0.66[20]	0.72
		0.5[14] 0.60[12] 0.60[11]	0.5−0.6[28]	
	(111) H	1.22,[13] 1.24, 1.25[8]	1.16, 1.21, 1.23[24]	1.44
		1.23[9], 1.21[2]	1.14, 1.19, 1.15[25]	
f (meV)	(100) H	⊥ 50−51.44[6]		44.51
	(110) H_3	⊥ 63, 65[17]		77.44
		62.0−70.7[18]		
		∥ 45−47[17] ?		32.57, 28.63
	(110) LB	⊥ 72[17] ?		45.12
	(111) H	65.7[40]		72.44
		66−67[15,16]		
	(711)H_4	⊥ 51−54[3]		43.68−44.00 (H_1−H_3)
	(711)H_3	⊥ 62−67[3]		70.11 (H_4)
E_b (eV)	(100) H	4.42[35] 4.55[37]	4.72−5.20[1]	4.90
		4.40, 4.57[34], 4−6.4[21]	4.78, 4.55[22]	
	(111) H	4.42[38] 4.40[36]	4.60−4.77[23] 4.42[22]	4.23
		4.98−6.24[39]	5.22, 4.93, 4.38[24]	
			5.03, 4.85, 4.24[22]	

top to top, and has a symmetrical zigzag along the [1$\bar{1}$0] direction, so it is the roughest of the low-index surfaces. From the results shown in Table 2, both LB and H_3 are surface adsorption states with $\lambda = 0$, SB is the surface diffusion transitional state between two H_3 sites, the H and T sites are surface diffusion maximum points, and S (not shown in Figure 1) is the surface diffusion transitional state between LB and H_3. To accurately show the potential energy surface (PES) for the adsorption and diffusion of O atoms on Rh(110), we scanned it at a height of 0.05 Å above the surface. The results are shown in three dimensions in Figure 3a.

Compared with the H site on Rh(111), the geometrical symmetry of H_3 may be taken as a slightly distorted C_{3v} local geometrical symmetry. From our calculation results, the eigenvibration mode of 72 meV is perpendicular to the surface and corresponds to A_1 irreducible representation. Because of distortion, the degenerate E irreducible representation decays and then splits into two 1D irreducible representations with eigenvibrations of 29 and 26 meV. Nevertheless, the split is so trivial that it is very difficult to be identified by experiments. The vibration mode of 29 meV is the one parallel to the surface for O atoms along the [001] direction, and the 26 meV is the one parallel to

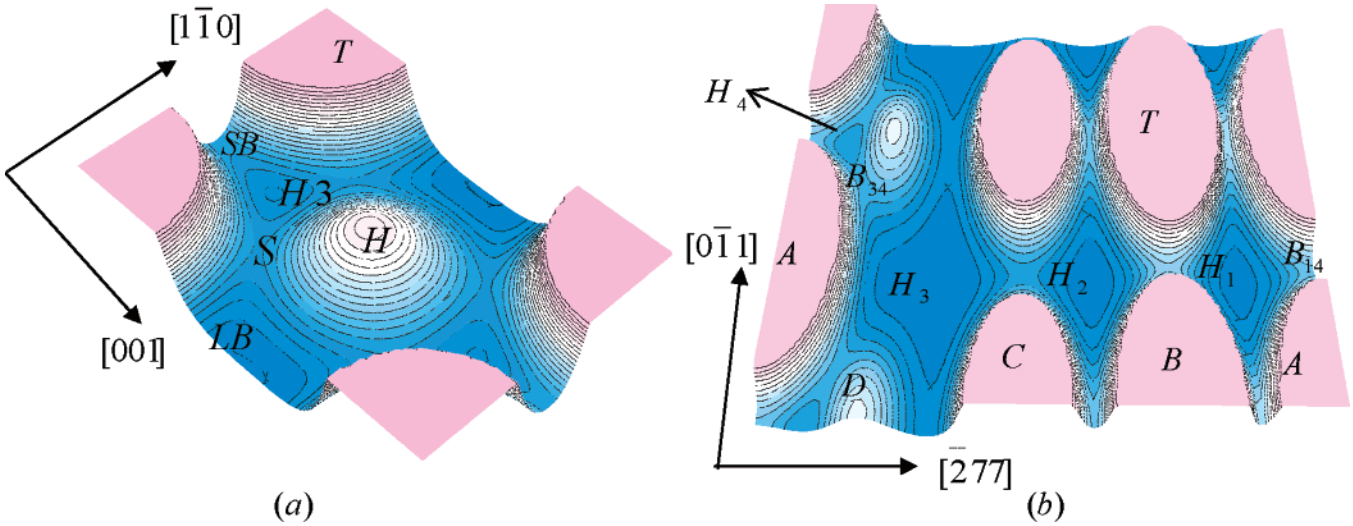

Figure 3. PES contour of O atom on Rh(711) crystal cell (a) O−Rh(110), $z = 0.005$ nm (b) O−Rh (711), $z = 0.02$ nm.

the surface along the [1$\bar{1}$0] zigzag direction. The geometrical symmetry of LB is C_{2v}, and the eigenvibration of 45.12 meV is perpendicular to the surface and corresponds to A_1 irreducible representation. The eigenvibration of 101 meV along the [001] direction and 19 meV along the [1$\bar{1}$0] zigzag direction are both parallel to the surface. They correspond to B_1 and B_2 irreducible representations, respectively, and the latter is a low-frequency vibration. As shown in Table 3, the critical characteristics of this work, such as the binding energy, adsorption height, and bond length, agree with the results in related studies.[10−14,20,28]

However, this work contradicts the conclusion of Alfe[17] et al. for the assignment of the vibration mode and the vibration frequency (indicated in Table 3 as Å). As mentioned in the Introduction, Alfe[17] et al. assigned 63 meV to the perpendicular vibration frequency of the 3-fold state on the basis of conclusions taken from Root et al.[15,16] Alfe[17] et al. assigned 45 meV to the parallel vibration frequency of the 3-fold state according to the equation for the frequencies of the perpendicular and parallel motions of an adatom in a 3-fold site.[29] At the same time, they[17] assigned 72 meV to the perpendicular vibration frequency of the LB site but thought that the parallel vibration frequency was not observed because of being annihilated. Regarding the fact that only 65 meV appeared when the (2 × 2) p2mg phase was formed, they interpreted that the parallel vibration frequency was annihilated because the O atom was imbedded deeply in the (1 × 2) trough. In addition, Cautero[18] et al. merely presented the value of the vibration frequency but did not assign it. This work gives a reasonable assignment of the vibration mode and the vibration frequency (in Table 3) by combining our theoretical calculations with their experimental data.

From the binding energy figures of Table 2, the H_3 site is shown to be the most steady state. So the O atom preferably resides on the H_3 site but not on the 4-fold[28] site nor on the LB[17] site at lower coverage. The experimental results of 72[17] and 68.2−70.7 meV[18] are consistent with the perpendicular vibration frequency of 77.44 meV on the H_3 state in this work.

O atoms tend to transfer both ways between H_3 and LB sites for the following reasons. The two binding energies of the H_3 and LB sites are contiguous (0.01 eV). The LB−S−H_3 channel is the lowest-energy diffusion location with potential energy barriers of only 0.02 and 0.03 eV. In addition, the parallel vibration of of the O atoms at the LB and H_3 sites are along the [1$\bar{1}$0] direction. Therefore, the O atom will occupy both the H_3 and LB sites with increasing coverage. So the experimental vibrations[17] of 63 (65) meV and 45 (47) meV should be assigned to the perpendicular vibration frequency of H_3 and LB, respectively. The calculated results in this work do not support the assignment of 45 (47) meV by Alfe.[17]

Alfe et al.[17] assigned 63 (65) and 45 (47) meV to the perpendicular and parallel vibration frequency of H_3 site, respectively. Because additional data of 65.7 and 66.9 meV by the loss spectra technique[15,16] of the O−Rh(111) system has been observed, it is easy to appoint it to the perpendicular vibration frequency of H_3. It is correct that Alfe[17] assigned 63 (65) meV to the perpendicular vibration frequency of H_3. Later, however, they assigned the 45 meV vibration frequency as parallel based on the equation for the frequencies of the perpendicular and parallel motions of an adatom in a 3-fold site.[29] Their conclusions are in agreement with the perpendicular and parallel vibration frequencies of H_3 are 72 and 50 meV, respectively, in this work. Compared with the H site on Rh-(111), the geometrical symmetry of H_3 is like the slightly distorted C_{3v}, and the parallel transformation data of H_3 are listed in this work; however, the experiment [17] concerned the perpendicular vibration frequency and ignored the transformation of parallel vibration frequency. Additionally, it is reasonable to assign 62.0−70.7 meV[18] to the perpendicular vibration frequency of H_3.

The binding energies of the O−Rh low index surfaces (see Table 2) are in the following order: (111) < (110) < (100), which is the same as the results in our study of O−Cu systems.[31] This result shows that the binding energies of the adsorption systems are independent from the roughness of the surface.

2.4. O-Rh(711) System. The Rh(711) surface is a more complex, intricate zigzag stepped surface constituted by the (100) terrace and (111) step as shown in Figure 2. The crystal cell of Rh(711) has a C_1 local geometrical symmetry. There are three 4-fold sites on the (100) terrace and one 3-fold site on the (111) step (see Figure 2). There are three kinds of nonequivalent critical points in the crystal cell of the system. First the 4-fold sites, H_1, H_2, and H_3, and the 3-fold site, H_4 (see Figure 3), are surface adsorption states with $\lambda = 0$. Second, the bridge sites are the surface diffusion transitional states with $\lambda = 1$. B_{14} is between H_1 and H_4, B_{34} is between H_3 and H_4, and the rest are between the adjacent 4-fold sites. Finally, the top sites, T, located at the tops of the A, B, C, and D layers are the surface diffusion maximum points with $\lambda = 2$. The characteristics of these three critical points are listed in Table 2. To accurately show the potential energy surface (PES) for

the adsorption and diffusion of O atoms on Rh(711), we scanned it at a height of −0.2 Å above the surface. The results are shown in three dimensions in Figure 3b.

Research on the O−Rh(711) system is rare both in experimentation and in theory; only the experimental study of Belton[3] et al. has been published. However, they were puzzled by their results. The 3-fold site on the (110) step is customarily regarded as the active site, but their conclusion that O atoms resided in the 4-fold sites on the (100) terrace in their experiment puzzled them. From Table 2 and Figure 3b, the critical characteristics of all of the 4-fold sites, H_1, H_2 and H_3, are very similar. However, the critical characteristics of the H_3 site, which is closest to the step, does change comparatively because of the influence of the step. Comparing all of the binding energies, the H_3 site is shown to be the most stable.

The local geometrical symmetries of the 4-fold states are slightly distorted C_{4v} patterns. The eigenvibration of 43.98, 44.00, and 43.68 meV correspond to the full-symmetrical A_1 irreducible representation and this mode is perpendicular to the surface. Owing to distortion, the degenerate E irreducible representation decays and splits into two 1D irreducible representations. The vibration mode of 73.87, 73.75, and 71.05 meV are parallel to the surface along the $[\bar{2}77]$ direction, whereas 73.54, 72.43, and 73.43 meV are parallel to the surface along the $[01\bar{1}]$ zigzag groove direction. The vibration properties of H_1, H_2, and H_3 are similar to those of the 4-fold states on O−Rh(100).

The local geometrical symmetries of 3-fold state H_4 may be regarded as a slightly distorted C_{3v} local geometrical symmetry. The eigenvibration of 70.11 meV obtained from our calculation is perpendicular to the surface, whereas the eigenvibrations of 50.23 and 46.12 meV are parallel to the surface. Apparently, the vibration properties of the H_4 state are similar to those of the 3-fold states on O−Rh(111) on the whole. Yet the fact that the terrace is so long actually affects the binding energy of the H_4 state. From the data shown in Table 2, the binding energy of 3.80 eV is obviously lower than that of the H state on Rh(111) and is the lowest of the O−Rh(711) system, supporting our conclusion that H_4 is metastable.

To find the channels of diffusion, we calculated the potential energy surface. The methods of determining diffusion properties of low index surfaces used in this work have been previously used successfully in our works on O−Cu,[31] O−Pd,[32] O−Ni,[33] and so forth. Table 2 reveals that the energy barriers for surface diffusion of O atoms on O−Rh(100) and O−Rh(111) systems, which possess only one adsorption state each, are both greater than 0.5 eV. This large energy barrier hinders the surface diffusion of O atoms. For the unique adsorption system O−Rh(110), which possesses two adsorption states, the low energy barrier for surface diffusion is between H_3 and LB, which induces the lowest-energy diffusion channel along the $[1\bar{1}0]$ zigzag groove direction. From the 3D illustration in Figure 3b, the 4-fold states, H_1, H_2, and H_3, and the 3-fold state, H_4, are the surface adsorption states. There are lowest-energy diffusion channels such as the H−B−H channel between these adsorption states. Through the calculation results, the diffusion barriers between 4-fold states are too high (>1 eV), whereas the diffusion between the 3-fold and 4-fold states is relatively moderate. The diffusion channel of $H_3-B_{34}-H_4$ is (1.59, 0.31 eV); namely, the diffusion potential energy barrier from H_4 to H_3 is 0.31 eV and is 1.59 eV in reverse, and therefore the 3-fold adsorption state, H_4, is defined as a metastable adsorption state. Comparatively, the diffusion in $H_1-B_{14}-H_4$ (1.67, 0.62 eV) is hard to carry out but is easier than that between the 4-fold states. Although the (111) step is the active site for the dissociation of O_2, the dissociated O atoms probably reside on the 3-fold site first, and then easily diffuse to adjacent H_3 sites. Thus, the 3-fold state, H_4, only adsorbs O atoms at high coverage.

As a result, the prediction that O_2 molecules dissociate on the (111) step in the first place and then diffuse hastily to the 4-fold sites, which was put forward by Belton et al.,[3] is agreed with and further explained in this work. The results in this work indicate that the step is still the active site, but not the most stable adsorption site. This conclusion eliminates the previous contradictions. From what has been mentioned above, the results in this work demonstrate and support the experimental results [3] by and large. Specifically, the fact that dissociated oxygen atoms are adsorbed in the 3-fold states on the (111) step with the perpendicular vibration frequency of 70.11 meV agrees with the experimental results.[3]

3. Conclusions

This work describes the interaction between O atoms and rhodium surfaces and studies the total critical characteristics of the O−Rh system by the 5-MP method.

3.1. In the O−Rh(100) system, only a 4-fold adsorption state exists on Rh(100). The state produces the perpendicular vibration frequency of 44.51 meV, and this frequency agrees with the experimental results.[6]

3.2. A 3-fold hollow site is the stable adsorption state in the O−Rh(111) system. The results in this work not only agree with the vibration frequencies in the experimental results, but also assign the frequencies[15,16] to the corresponding adsorption sites.

3.3. For the O−Rh(110) system, a pseudo-3-fold site is the stable adsorption state that is occupied steadily by O atoms at low coverage first. At the same time, the perpendicular vibration frequency of 72 meV, similar to an HREELS experiment,[17] was obtained. At high coverage, the O atom is located at the LB site and produces a perpendicular vibration frequency of 45.12 meV. By analyzing the critical properties of the 3-fold site, the experimental vibration frequencies[17,18] were assigned (Table 3).

3.4. For the O−Rh(711) stepped system, the step site is the active site but not the most stable adsorption site. The results indicate that the 3-fold site is the metastable adsorption state and the 4-fold sites are the stable adsorption states. The adatoms diffuse easily from 3-fold to 4-fold states at low coverage; therefore, O atoms are absorbed on the 4-fold state on the (100) terrace. With increasing coverage, the O atoms will become located on the 3-fold site on the (111) step. All of these results agree perfectly with the experimental results[3] and also interpret well the discrepancy between the experimental results[3] and the idea that the step is the active site.

Acknowledgment. The authors greatly appreciate very helpful comments on the manuscript by Mr. Scott Murphy. We express our sincere thanks to the Community of Shandong Natural Science Foundation (no. Y2002B09) for their support.

References and Notes

(1) Hansen, E.; Neurock, M. *Surf. Sci*. **1999**, *441*, 410−424.
(2) Greber, T.; Wider, J.; Wetli, E.; Osterwalder, J. *Phys. Rev. Lett.* **1998**, *81*, 1654−1657.
(3) Belton, D. N.; Fisher, G. B.; DiMaggio, C. L. *Surf. Sci*. **1990**, *233*, 12−26.
(4) Baraldi, A.; Cerdá, J.; Martín-Gago, J. A.; Comelli, G.; Lizzit, S.; Paolucci, G.; Rosei, R. *Phys. Rev. Lett.* **1999**, *82*, 4874−4877.
(5) Oed, W.; Dötsch, B.; Hammer, L.; Heinz, K.; Müller, K. *Surf. Sci*. **1988**, *207*, 55−65.
(6) Dubois, L. H. *J. Chem. Phys.* **1982**, *77*, 5228−5233.

(7) Castner, D. G.; Sexton, B. A.; Somorjai, G. A. *Surf. Sci.* **1978**, *71*, 519−540.
(8) Over, H.; Schwegmann, S.; De Renzi, V.; Ertl, G. *Surf. Sci.* **1997**, *375*, 91−106.
(9) Wong, P. C.; Hui, K. C.; Zhou, M. Y.; Mitchell, K. A. R. *Surf. Sci.* **1986**, *165*, L21−L25.
(10) Comelli, G.; Dhanak, V. R.; Kiskinova, M.; Paolucci, G.; Prince, K. C.; Rosei, R. *Surf. Sci.* **1992**, *260*, 7−13.
(11) Gierer, M.; Over, H.; Ertl, G. *Surf. Sci.* **1993**, *297*, L73−L93.
(12) Van Hove, M. A.; Batteas, J. D.; Barbieri, A.; Starkey, E. K.; Somorjai, G. A. *Surf. Sci.* **1995**, *339*, 142−150.
(13) Mitchell, K. A. R.; Wong, K. C.; Liu, W. *Surf. Sci.* **1996**, *360*, 137−143.
(14) Comicioli, C.; Dhanak, V. R.; Comelli, G.; Astaldi, C.; Prince, K. C.; Rosei, R.; Atrei, A.; Zanazzi, E. *Chem. Phys. Lett.* **1993**, *214*, 438−444.
(15) Root, T. W.; Fisher, G. B.; Schmidt, L. D. *J. Chem. Phys.* **1986**, *85*, 4679−4686.
(16) Root, T. W.; Fisher, G. B.; Schmidt, L. D. *J. Chem. Phys.* **1986**, *85*, 4687−4695.
(17) Alfe, D.; Rudolf, P.; Kiskinova, M.; Rosei, R. *Chem. Phys. Lett.* **1993**, *211*, 220−226.
(18) Cautero, G.; Astaldi, C.; Rudolf, P.; Rosei, M. K. *Surf. Sci.* **1991**, *258*, 44−54.
(19) Norris, A. G.; Schedin, F.; Thornton, G.; Dhanak, V. R.; Turner, T. S.; McGrath, R. *Phys. Rev. B* **2000**, *62*, 2113-2117.
(20) Baroni, S.; Stokbro, K. *Surf. Sci.* **1997**, *370*, 166−178.
(21) Mercer, J. R.; Finetti, P.; Scantlebury, M. J.; Beierlein, U.; Dhanak, V. R.; McGrath, R. *Phys. Rev. B* **1997**, *55*, 10014−10021.
(22) Loffreda, D.; Simon, D.; Sautet, P. *J. Chem. Phys.* **1998**, *108*, 6447−6457.
(23) Chen, M.; Bates, S. P.; van Santen, R. A.; Friend, C. M. *J. Phys. Chem. B* **1997**, *101*, 10051−10057.
(24) Ganduglia-Pirovano, M. V.; Scheffler, M. *Phys. Rev. B* **1999**, *59*, 15533−15543.
(25) Ganduglia-Pirovano, M. V.; Reuter, K.; Scheffler, M. *Phys. Rev. B* **2002**, *65*, 245426−245434.
(26) Alfè, D.; de Gironcoli, S.; Baroni, S. *Surf. Sci.* **1999**, *437*, 18−28.
(27) (a) Rahman, T. S.; Black, J. E.; Mills, D. L. *Phys. Rev. B* **1981**, *25*, 883−906. (b) Rahman, T. S.; Black, J. E.; Mills, D. L.; *Phys. Rev. Lett.* **1981**, *46*, 1469−1472.
(28) Sun, C. Q. *Surf. Sci.* **1998**, *398*, L320−L326.
(29) Ibach, H.; Mills, D. L. *Electron Energy Loss Spectroscopy and Surface Vibrations*; Academic Press: New York, 1982.
(30) Hopster, H.; Ibach, H. *Surf. Sci.* **1978**, *77*, 109−117.
(31) Wang, Z. X.; Tian, F. H. *J. Phys. Chem. B* **2003**, *25*, 6153−6161.
(32) Wang, Z. X.; Jia, X. F.; Tian, F. H.; et al. *Chin. J. Chem*., in press.
(33) Wang, Z. X.; Qiao, Q. A.; Chen, S. G. et al. *Surf. Sci.* **2002**, *517*, 29−42.
(34) Kose, R.; Brown, W. A.; King, D. A. *Surf. Sci.* **1998**, *402−404*, 856−860.
(35) Shustorovich, E.; Bell, A. T.; *Surf. Sci.* **1993**, *289*, 127−138.
(36) Fisher, G. B.; Schmieg, S. J. *J. Vac. Sci. Technol.* **1983**, *A1*, 1064.
(37) Brown, W. A.; Kose, R.; King, D. A. *Chem. Rev.* **1998**, *98*, 797.
(38) Shustorovich, E. *Adv. Catal.* **1990**, *37*, 101.
(39) Root, T. W.; Schmidt, L. D.; Fisher, G. B. *Surf. Sci.* **1983**, *134*, 30−45.
(40) Somorjai, G. A.; Semancik, S.; Haller, G. L.; Yates, J. T. *Appl. Surf. Sci.* **1982**, *10*, 546.